AIAA 82-4254

Bifurcation Analysis of Nonlinear Aircraft Dynamics

James V. Carroll* and Raman K. Mehra†
Scientific Systems, Inc., Cambridge, Massachusetts

A new approach is presented for analyzing nonlinear and high-α dynamic behavior and stability of aircraft. This approach involves the application of bifurcation analysis and catastrophe theory methodology to specific phenomena such as stall, departure, spin entry, flat and steep spin, nose slice, and wing rock. Quantitative results of a global nature are presented, using numerical techniques based on parametric continuation. It is shown how our methodology provides a complete representation of the aircraft equilibrium and bifurcation surfaces in the state-control space, using a rigid body model with aerodynamic controls. Also presented is a particularly useful extension of continuation methods to the detection and stability analysis of stable attracting orbits (limit cycles). The use of this methodology for understanding high-α phenomena, especially spin-related behavior, is discussed.

I. Introduction

TRENDS in fighter aircraft design over the past few decades have resulted in configurations noted for their high speed and performance capability. The cost of achieving this capability has been a drastic, often fatal loss of positive control of the aircraft as the pilot operates at or near the extremes of the flight envelope. This is especially true for aircraft motion at high angles of attack (α), where large deviations both in the state and control variables limits the application of the usual linearized analysis techniques. There is a conspicuous lack of techniques for analyzing global stability and large maneuver response of aircraft. While certain phenomena (e.g., roll coupling) have been analyzed in an isolated manner, there exists a clear need for a unified approach to analyze systematically global aircraft behavior at high α.

A suitable methodology for global stability analysis would, in addition to providing quantitative, global stability information, also contribute toward safer piloting procedures, control system design, stability augmentation, and aircraft model structure determination and design. The method should also be able to predict and explain such high-α phenomena as discontinous motion (jumps), limit cycle behavior, and hysteresis effects. There is a particular need for a more complete understanding of limit cycle phenomena, because it is a critical part of high-α motion for all of the aircraft we have investigated.

The bifurcation analysis and catastrophe theory methodology (BACTM) approach has been developed to accomplish the above objectives. It can make consistent and accurate high-α stability predictions for quasistatic control motions. BACTM owes its success to several factors, including: 1) the use of wind tunnels designed explicitly for spin testing and the flight testing of radio-controlled scale models are but two of several approaches which have resulted in aero data which are more realistic for high-α flight regimes[1,2]; 2) the development of relatively inexpensive and efficient simulation facilities, which capably generate the full six degree-of-freedom results required for a high-α analysis; and 3) the development of the underlying theory for BACTM. This includes not only recent results in the fields of topology, qualitative theory of differential equations, differential geometry, structural stability, bifurcation analysis, and catastrophe theory.[3,4] It also includes the development of advanced mathematical techniques for stability analysis[5] and parameter identification[6] which can aid in the task of developing adequate high-α models. Finally, it includes new computational techniques.[7-10]

The advances reported in this paper resulted from recognizing that discontinuous and limit cycle phenomena at high α could be analyzed using the new theoretical results.[11] Independent work by others, such as Schy and Hannah[12] and Young et al.[13] have supported this observation, and our results have not only confirmed our original conjecture, but have also revealed new dynamic phenomena at high α. A major step in the realization of BACTM as an effective tool for high-α stability analysis has been the implementation of continuation methods for the solution of the aircraft equations required by BACTM. The continuation technique used here is derived from the work of several researchers.[7,8,14-16] It has led to successful application of the theory to real-world systems of complex structure and high order, by translating the BACTM equations into a form amenable to solution on digital machines. The equilibrium and bifurcation surfaces, as well as quantitative limit cycle information, are all generated by our continuation algorithms.

The next section discusses high-α dynamics and presents the simulation equations for the two aircraft models investigated here: a variable sweep fighter (aircraft F) and a swept-wing fighter (F-4). Section III discusses briefly the underlying principles of BACTM and then describes how parametric continuation techniques work. Section IV discusses specific results for the F-4 and aircraft F systems, and Sec. V summarizes the main results and presents our conclusions.

II. High-α Dynamics of Aircraft

Traditional aircraft stability analysis and control system synthesis have depended heavily on techniques involving linearization. This approach is very advantageous where applicable, as the analysis is not only more standardized, but also the system order is greatly reduced due to decoupling effects. As aircraft became faster and more maneuverable, however, it has become more difficult to justify linear methods in many critical flight regimes. This is especially true in the case of high-α motions, particularly so since airframe modifications resulting from the desire to reduce drag (hence increasing speed) and increase maneuverability quite often compromise handling and performance characteristics. As an example, the stubby, thin wings of most modern fighter aircraft reduce drag, but the consequently smaller value of

Received April 27, 1981; revision received April 5, 1982.

*Manager, Aerospace Sciences Division. Member AIAA.
†President.

axial inertia enhances roll coupling and autorotational effects. These are undesirable responses which are the consequence of the greater role that certain nonlinear terms achieve in the equations. Such responses are often counterintuitive as well, often inducing the pilot to control actions which worsen the situation.

Equations of Motion

The basic aircraft equations of motion for BACTM analysis are given by the general form

$$\dot{x}=f(x,\delta) \tag{1}$$

where f is the mapping f: $R^n \times R^3 \to R^n$ and $x \epsilon R^n$, $\delta \epsilon R^3$ ($\delta \triangleq [\delta a, \delta e, \delta r]$). For a rigid body aircraft with constant mass in a constant-gravity environment, Eq. (1) expands to[17]

$$\dot{p}=-\frac{I_z-I_y}{I_x}qr+\bar{q}\frac{Sb}{I_x}C_l \tag{2}$$

$$\dot{q}=\frac{I_z-I_x}{I_y}pr+\bar{q}\frac{Sc}{I_y}C_m \tag{3}$$

$$\dot{r}=-\frac{I_y-I_x}{I_z}pq+\bar{q}\frac{Sb}{I_z}C_n \tag{4}$$

$$\dot{\alpha}=q+\left[\left(\frac{\bar{q}S}{mV}C_z+\frac{g}{V}\cos\theta\cos\phi-p\sin\beta\right)\cos\alpha - \left(\frac{\bar{q}S}{mV}C_x-\frac{g}{V}\sin\theta+r\sin\beta\right)\sin\alpha\right]\sec\beta \tag{5}$$

$$\dot{\beta}=\left(\frac{\bar{q}S}{mV}C_y+\frac{g}{V}\cos\theta\sin\phi\right)\cos\beta - \left[\left(\frac{\bar{q}S}{mV}C_x-\frac{g}{V}\sin\theta\right)\sin\beta+r\right]\cos\alpha - \left[\left(\frac{\bar{q}S}{mV}C_z+\frac{g}{V}\cos\theta\cos\phi\right)\sin\beta-p\right]\sin\alpha \tag{6}$$

$$\frac{\dot{V}}{V}=\left(\frac{\bar{q}S}{mV}C_z+\frac{g}{V}\sin\theta\right)\cos\alpha\cos\beta+\left(\frac{\bar{q}S}{mV}C_y + \frac{g}{V}\cos\theta\sin\phi\right)\sin\beta+\left(\frac{\bar{q}S}{mV}C_z + \frac{g}{V}\cos\theta\cos\phi\right)\sin\alpha\cos\beta \tag{7}$$

The nondimensional force moment coefficients C_x, C_y, C_z, C_l, C_m, and C_n are defined in the usual way. These coefficients are linear functions of the aerodynamic controls, and are tabular functions of the angles of attack and sideslip. Our analysis did not cover Mach-dependent aero data. In Eqs. (2-7), the body axis coordinatization is assumed to be into body principal axes, so that all cross products of inertia are zero. Also, the origin of this axis system is the vehicle center of mass, so that no gravity torques exist in (p,q,r). Equations (2-7) represent a set of nonlinear, autonomous, ordinary differential equations describing rotational and translational accelerations on the vehicle. Where gravity plays an important role (e.g., spin motion), it is necessary to add two kinematic equations for pitch and roll,

$$\dot{\theta}=q\cos\phi-r\sin\phi \tag{8}$$

$$\dot{\phi}=p+(q\sin\phi+r\cos\phi)\tan\theta \tag{9}$$

BACTM is capable of analyzing nonautonomous systems, so that fuel depletion and time-varying feedback effects, for example, can be studied, but the basic results do not require this added complexity. The elements of x, the state variable, are $p,q,r,\alpha,\beta,V,\theta$, and ϕ so that the coupled dynamic system is of the eighth order. The advantage of BACTM and the continuation methods is that no further simplification is required beyond a sufficiently smooth function f, whereas other techniques often require several levels of simplification. Note how relatively small values of I_x, the axial inertia term, produce larger values for the nonlinear term in Eqs. (2-4) and effectively couple longitudinal motions (pitch) into the lateral motions, as we indicated above.

The aerodynamic coefficients are derived from static, forced oscillation, and rotary balance wind tunnel data. These data are tabular, and are interpolated by means of cubic spline function approximations.

Aircraft Models

Aircraft F is a variable-sweep fighter whose aero-data have been altered somewhat in order to study certain spin motions.[18] Its aero data base is considerably smaller than that of the F-4, yet aircraft F nonetheless has been extremely useful in developing the BACTM algorithms and in providing initial spin analysis results. We discuss spin behavior and its characteristics in more detail below.

The selection of the F-4 was motivated by the availability of its high-α aero and flight test data base and by the desire to investigate an actual aircraft. Also, the F-4 has a history of being excessively difficult to recover from certain types of spin motion,[19] and so it is of practical importance to seek better understanding of its high-α behavior. Digital representation of the aircraft dynamics is crucial to achieving credible results at high α. However, because it is difficult to obtain reliable aerodynamic data for general maneuvers at high α, one should not rely on the quantitative merit of stability predictions made with BACTM.

High-α Motion

Many of the phenomena encountered in flight tests—wing rock, nose slice, prestall buffeting, stall, poststall departure, and spin—are oscillatory in nature, adding emphasis to the application of limit cycle analysis and Hopf and global bifurcation theory to high-α dynamics (see Sec. III). Wing rock is a condition of high-frequency roll rate oscillation, and is a stall/poststall extension of the prestall buffeting condition. It again represents high-α longitudinal-lateral coupling effects. This condition is the result of a Hopf bifurcation (explained below), as δe decreases to its minimum value. Nose slice is a similar phenomenon, but contains more yaw rate in the motion than does wing rock. It is also a condition which is prominent near stall values of α. Stall and poststall departures are transient motions, and usually represent a transition phase between trim equilibrium and high α, attracting stable orbits (limit cycles) such as spin. Spin is a poststall condition featured by very high, persistent values of α and excessive yaw rate.

The above flight conditions are qualitative. Our BACTM analysis has verified their presence quantitatively, as well as other types of high-α motion, some of which are combinations of the above.

III. Continuation Methods

The continuation methodology which we will discuss in this section is the bridge by which the abstract mathematical results from topology, bifurcation analysis, and catastrophe theory are joined to generate global stability results for aircraft dynamic systems at high α. Continuation methods effectively broaden the scope of application of the theory. Before discussing continuation, we present a brief overview of the BACTM approach.

BACTM allows one to study the global behavior of nonlinear systems in an $(n+m)$ dimensional space where n is the number of state variables and m is the number of control variables. The BACTM methodology is based on four theorems: center manifold theorem, classification theorem of elementary catastrophes, Hopf bifurcation theorem, and global implicit function theorem. A discussion of these theorems and a bibliography are found in Ref. 20. This reference also demonstrates that Thom's classification theorem[4] may be applied to constant coefficient aircraft models.

The application of this methodology to dynamic systems enables global characterization of stability boundaries, domains of attraction, bifurcation and jump surfaces, and limit cycles. This characterization requires the generation of the system equilibrium and bifurcation surfaces, and only in simple cases is it possible to do this analytically. It is for this reason that we turn to continuation methods, as well as for reasons of efficiency, accuracy, and ability to deal readily with singularities.

Continuation methods utilize results from topology and differential calculus. They deal with the problem of solving

$$g(x,\lambda)=0 \tag{10}$$

for the state variables x as a function of the parameter λ. We note the similarity of g in Eq. (10) to f in Eq. (1): in fact, the generation of equilibrium surfaces involves solving for points in R^{n+m} where $\dot{x}=0$, so that in this case, $f=g$. Our applications of continuation methods at this time consist of computing equilibrium surfaces, bifurcation surfaces (defined later), and limit cycle solutions (also defined and explained below). In each of these cases, x is an element of a finite-dimensional space and λ is a real parameter, $\lambda \epsilon R^1$. The theory is actually more general and x may be an element of an infinite-dimensional Banach space B, with $\lambda \epsilon R^m$. The case $x \epsilon B$ occurs in trajectory optimization,[21] structural,[22] and chemical reaction[23] problems.

By solving Eq. (10) for the spatial trajectory $x(\lambda)$ it is possible to determine x at some λ_1, say, based on an initial solution $x(\lambda_0)$. It is not necessary that $|\lambda_1-\lambda_0|$ be infinitesimal, as perturbation methods require. In fact, the usual procedure is to choose λ_0 solely for the purpose of finding relatively easily a solution to Eq. (10) and then "continue" the solution to λ_1, which would represent a physically realistic value, but for which analytical solution of Eq. (10) is difficult. To generate an equilibrium surface, we seek not only solutions at λ_0 and λ_1 (for the aircraft problem $\lambda \epsilon \delta$), but λ at all points in between, and these are provided as a byproduct of the continuation method.

Our approach to solution by continuation is to combine the methods of Lahaye[15] and Davidenko.[14] The former begins with a solution at $\lambda=\lambda_0$, using $x(\lambda_{i-1})$ as the initial guess in a Newton-Raphson iteration at λ_i, $i>0$. Davidenko differentiated Eq. (10) with respect to λ to obtain

$$G(x,\lambda)\frac{\partial x}{\partial \lambda}+\frac{\partial g}{\partial \lambda}(x,\lambda)=0 \tag{11}$$

which is usually integrated readily from λ_0 to any λ_1 (exceptions are noted below). In this equation, the matrix

$$G \triangleq \frac{\partial g}{\partial x} \tag{12}$$

The algorithm uses Davidenko's method for prediction and Lahaye's method as a corrector step. In this way, the methods are complementary, as for example, Davidenko's method does not require as close an initial guess as Lahaye's, but is less accurate. At each solution point, the eigenvalues of G are checked to provide local stability information.

As implied above, solution of Eq. (11) proceeds normally at most points (x,λ). The exceptions are where the matrix G is singular. By application of concepts from topology, the continuation method can deal with singularities, as we now show, utilizing results of Keller[7] and Kubicek.[9]

G is singular at a *limit point* or at *bifurcation points*. A limit point in state-parameter space occurs where the solution curve begins to "fold back" on itself, that is, λ is not monotonic; a *simple bifurcation* occurs where two curves intersect and a *general bifurcation* where more than two curves intersect. Some authors[24] classify a limit point as a bifurcation point also, since the stable attractor is annihilated by an unstable attractor. Other types of bifurcations are global bifurcations (a stable attracting orbit or limit cycle annihilated by an unstable one), Hopf bifurcation (a stable attractor or fixed point changing into a limit cycle as λ changes), and the singular perturbation bifurcation [in which $x(\lambda)\to\infty$ as $\lambda\to\lambda_1$; this class of singularity is not encountered in our problem].

It is now convenient to rewrite Eq. (10) as

$$g[z(s)]=0 \tag{13}$$

where z is the $(n+1)$ vector (x,λ) and s a scalar arclength parameter. This emphasizes the fact that there is no distinction between λ and the x_i in the methods that follow. Since $g \epsilon R^n$ and $z \epsilon R^{n+1}$, the solution points generate a trajectory in R^{n+1}. At a limit point, the rank of the $n\times(n+1)$ matrix

$$\Gamma \triangleq \frac{\partial g}{\partial z}=\left[G \;\vdots\; \frac{\partial g}{\partial \lambda}\right] \tag{14}$$

is n, the same as for nonsingular G (hence, limit points are known as *weak singularities*). We exploit this by defining the arclength parameter s and reformulating our problem to one of solving for those points $z(s)\epsilon R^{n+1}$ which satisfy Eq. (13) as s varies. Davidenko's equation (11) is then modified to reflect the new independent variable s,

$$G\dot{x}+\frac{\partial g}{\partial \lambda}\dot{\lambda}=0 \tag{15}$$

where $(\dot{})\triangleq \mathrm{d}(\;)/\mathrm{d}s$.

Keller[7] shows that the Frechet derivative of the system [Eqs. (13) and (15)], which was expanded by introducing s, has similar features at regular and limit points and that, therefore, continuation around limit points is feasible. Heuristically, replacing λ, which ceases to be monotonic, with s restores regularity. Keller suggests several non-Euclidean arclength expressions ("normalizations"), but we have found success using the Euclidean one,

$$N(z,s)=\dot{z}_1^2+\cdots+\dot{z}_{n+1}^2-1=0 \tag{16}$$

The augmented Frechet derivative is $A \triangleq \partial(g,N)/\partial z$.

Kubicek[9] has introduced a numerical algorithm for continuing past limit points, based on Gaussian elimination with controlled pivoting; it is this algorithm which we have incorporated in BACTM. It exploits results obtained by Keller. Since Γ has rank n at a limit point, there must be at least one nonsingular Γ_k, where Γ_k is an $n\times n$ submatrix of Γ formed by eliminating the kth column of Γ, for $k\epsilon(1,n+1)$. (Note that $G \triangleq \Gamma_{n+1}$.) Equation (15) then may be rearranged

$$\Gamma_k[\dot{z}_i]_{i\neq k}+\frac{\partial g}{\partial z_k}\dot{z}_k=0 \tag{17}$$

Equation (17) is then solved for the $n\dot{z}_i$, $i\neq k$, in terms of $\dot{z}_k$, and $\dot{z}_k$ is found using Eq. (16). Sign ambiguity is resolved by choosing one of two possible directions for proceeding along the solution arc passing through λ_0. Column k represents the "singular" column at a limit point and the "most singular" column at regular points.

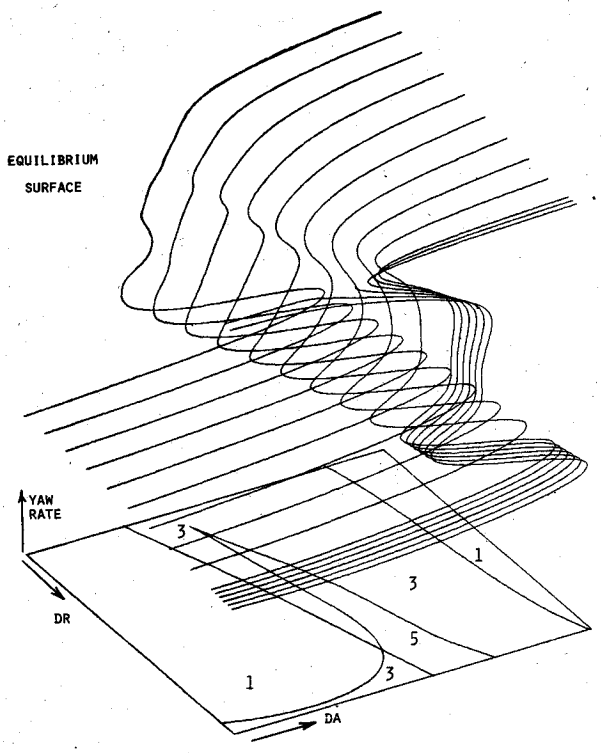

Fig. 1 F-4 equilibrium: bifurcation surfaces.

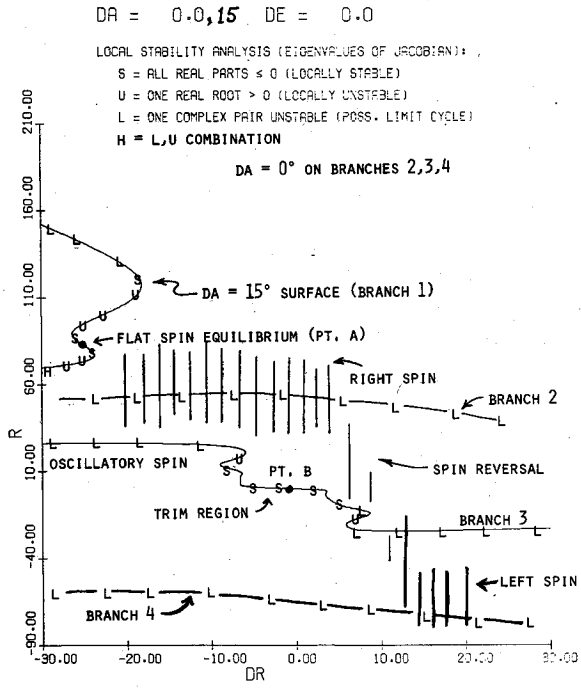

Fig. 2 Aircraft F spin recovery: equilibrium surfaces.

The controlled pivoting method of Gaussian elimination finds k as follows: Γ is scanned for the element with the largest magnitude. This element becomes the pivot about which elementary matrix operations are performed to reduce all elements in the column of the pivot to zero, except of course the pivot itself. The scan is repeated for a total of n times, each time ignoring rows and columns containing past-selected pivot elements. The unselected column is column k. Having obtained $\dot{z}$, it may be used in either the predictor or corrector algorithms. In the corrector (Newton), it is solved for as Δz ($\Delta z_k \equiv 0$). In the predictor, $\dot{z}$ is used in Adams-Bashforth variable order integration. Pivoting may be controlled by selective scaling of the columns of Γ.

At a bifurcation point, the method of Kubicek breaks down. This is because the rank of Γ is $(n-1)$ for a simple bifurcation point, or less (general bifurcation point). Keller[7] has developed an algorithm for detecting bifurcation points and for continuing along all branches emanating from them. It can be shown using Taylor expansions that, to second order at a simple bifurcation point, each intersecting branch is locally tangent to the subspace spanned by the eigenvectors associated with the zero eigenvalues of the $(n+1) \times (n+1)$ matrix $\Gamma^T\Gamma$. For a simple bifurcation point, there are two such eigenvectors and the plane they form is normal to the range space of Γ. Thus in this case, initial points to all four branches emanating from the simple bifurcation point z^* may be found by seeking zeroes of $g(z^*+\Delta z)=0$, where Δz has some small fixed-magnitude ϵ and lies in the above plane. The quantity ϵ should be large enough to avoid the numerical problems associated with z^*, yet small enough so that the Taylor approximations are reasonable.

Application of the Continuation Method

Here, we specify the three problems to which the BACTM continuation algorithm has been applied to the analysis of high-α dynamics of aircraft. Results are discussed in Sec. IV.

Equilibrium Surfaces

This is the system for which g in Eq. (13) becomes

$$g[x(s),\lambda(s)]=0 \tag{18}$$

where x are the aircraft state variables and λ is one of the aerodynamic controls (the other two are fixed while each equilibrium locus is generated). See Fig. 1 for a general example. Local stability information is obtained by examining the eigenvalues of $[\partial g/\partial x]$ in the usual manner. Global stability information is obtained by inspecting one or several relevant equilibrium surfaces generated by the above method. This will be discussed shortly, in relation to Fig. 2.

Bifurcation Surfaces

This is our designation for those manifolds resulting from the projection (sometimes called a catastrophe map[25]) of the limit points of the system (18) onto the control subspace R^m. This condition adds to Eq. (18) the additional requirement $\Delta \triangleq \det(G)=0$. Thus, g in Eq. (13) becomes

$$g[z(s)]=\{f[z(s)],\Delta[z(s)]\}=0 \tag{19}$$

where $g \epsilon R^{n+1}$, so that $z=(x,\lambda)^T \epsilon R^{n+2}$. We therefore select two of the aerodynamic controls to augment x, holding the third fixed, that is, $\lambda \epsilon R^2$. Every solution of Eq. (19) then generates a curve in two-dimensional control space (Fig. 1).

It should be mentioned that great care must be taken here in the computation of Γ, which now has size $(n+1)\times(n+2)$. G is still a submatrix of Γ, yet it must be evaluated much more often at each point, not only to produce Δ, but also to evaluate the $(n+2)$ vector $(\partial\Delta/\partial z)$. Our approach is to evaluate as many elements of Γ as possible analytically and to use splines to evaluate the last row of $(\partial\Gamma/\partial z)^T$ numerically. A spline fit is done for each z_i, requiring five evaluations at the points $(z_i \pm j\epsilon)$ for $j\epsilon(-2,2)$. Thus 4 $(n+2)$ evaluations of Δ (hence G) are needed every time Γ is evaluated, as well as one extra at $G(z)$, to fill out the rest of Δ.

Limit Cycle Continuation

A limit cycle is a nonlinear oscillation satisfying the condition

$$x(T;x_0)-x_0=0 \tag{20}$$

for some fixed $T\epsilon'(0,T_{max})$, $T_{max}<\infty$, where, in general,

$$x(t;x_0)=x_0+\int_{t_0}^{t} f(x,\delta,\tau)d\tau \tag{21}$$

Specifically, a motion satisfying Eq. (20) in R^n is called a closed orbit. For $n=2$, planar motion, this will be a limit cycle, but not every higher dimensional closed orbit is a limit cycle. A limit cycle differs from a linear oscillator in that there can exist only a countable number of limit cycles in the state space R^n, whereas there is an infinity of linear oscillatory solutions. Of the possible limit cycles, the stable attractors represent the ultimate condition of all motions whose initial conditions lie within its "domain of attraction," which is usually a finite region encompassing the limit cycle. Motions starting outside the domain of attraction of a limit cycle ultimately diverge from that limit cycle. An unstable limit cycle is one for which any neighboring trajectory not explicitly on the cycle ultimately diverges from it. Unstable limit cycles are not physically observable, but affect the dynamics, e.g., via global bifurcation.

Our goal is to find x_0 and $T(x_0)$ for system 1 such that Eq. (20) holds. We utilize results from Chua and Lin,[10] who provide a method for finding one (x_0,T_0) pair; however, we have expanded the scope of their method by incorporating it into the framework of continuation methods, so that we can generate a continuum of limit cycle points $x[T(s),\lambda(s)]$, as the continuation parameter λ is changed. This extension represents a significant advance over previously used methods of limit cycle detection and analysis. By invoking the robustness and globality of the continuation approach, it is possible to start where a known limit cycle exists, at λ_0, and continue λ to regions where solutions are difficult to obtain.

To apply the continuation method, g in Eq. (13) becomes

$$g[z(s)]=x\{T[z(s)];x_0[z(s)]\}-x_0[z(s)]=0 \tag{22}$$

Now $g\epsilon R^n$ and $z_{n+1}=\lambda$, one of the aerodynamic controls, so that one of the $n+1$ elements (x_0,T) must be dealt with. Details are in Ref. 10, which show a procedure for selecting an element of x as a fixed parameter for the corrector iterations. Use of double-precision arithmetic along with Adams-type integrators has resulted in the best combination of solution speed and accuracy for the integration algorithms.

Like equilibrium points, limit cycles are classified as stable or unstable depending on whether they are attracting or repelling. Unlike the fixed point case, however, the gradient of g as given by Eq. (22) does not directly yield stability information. We are more properly interested in the eigenvalues of

$$H=\frac{\partial x(T;x_0)}{\partial x_0} \tag{23}$$

The Jacobian matrix G is needed in the continuation process to iterate for solution points to Eq. (20). Once a solution point has been found, all but one column of H can be constructed readily from G at the solution point (details to be published shortly). It can be shown from topological concepts[26] that if all but one of the eigenvalues of H are less than 1 in magnitude, the limit cycle is stable. The remaining one is identically 1, because of the mapping implicit in Eq. (20). Similar results are obtained from Floquet analysis,[27] although the Floquet numerical technique is often troublesome.

IV. Application of BACTM to the Aircraft High-α Problem

Figure 2 shows a composite of four equilibrium branches which indicate how BACTM-generated equilibrium surfaces are used to understand and predict high-α behavior, in this case spin and spin recovery. It shows curves of equilibrium yaw rate r vs rudder δr for trim elevator ($\delta e=0$ deg). The letters along the curves indicate the local stability results as follows: S is a stable point (all eigenvalues of the linear part of f, i.e., the gradient of g in Eq. (18), have negative real parts), U a simple unstable point (one positive root), L an unstable complex pair, and H (lower part of branch 1) an LU combination. The S segments are known as stable attractors and motions beginning near them end up on them. The domain of attraction of such attractors is often delineated by the saddle points along with their separatrices (U segments). The vertical bars in Fig. 2 show the projection of steady-state yaw rate motion in $(r-\delta r)$ space.

All non-S segments are locally divergent; however, globally the motion may grow to a limit cycle (this is the expected result near an L segment; quantification of limit cycles is done by using the limit cycle continuation method discussed in Sec. III).

Jump phenomena occur at limit points. This is the manner in which one may escape an undesirable stable equilibrium such as the flat spin segment of branch 1. Equilibria on branch 1 exist for $\delta a=15$ deg; for the other branches shown, $\delta a=0$ deg. Rudder is increased from its spin value (-25 deg), changing the equilibrium from point A to a dynamic condition influenced by branch 2. As rudder goes positive, the attracting closed orbit near branch 2 is annihilated (global bifurcation at $\delta r=5$ deg) by an unstable one, and the motion becomes influenced by branch 3's stable attractor. If δr is held at a high positive value, the motion will ultimately be attracted to branch 4 (spin reversal); the desired result, return to trim at point B, is achieved by holding δr for a short time at 30 deg and then returning to trim as δr gets small. Figure 3 verifies that this strategy produces recovery. (In the course of jumping from branch 1 in Fig. 2, δa was changed to trim from 15 deg; the surfaces in this region were found to be rather insensitive to δe, so it was held at trim. This would be the initial control step in a recovery sequence.) Returning to Fig. 2, the size of the vertical bars indicates the amplitude of the limit cycle for the given δr value. The rudder was incremented in 2 deg steps, and held for 30 s at each step, from -20 to 20 deg. The pattern for decreasing δr is much different. Thus,

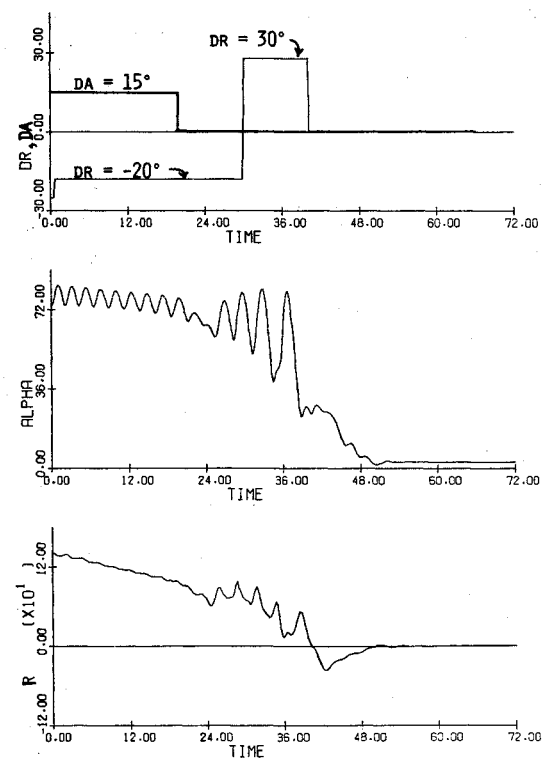

Fig. 3 Aircraft F spin recovery: time history.

hysteresis is a factor in studying this motion. We further point out that, because our analysis is limited to quasistatic control motions, the control strategy shown in Fig. 3 is typically suboptimal.

The F-4 model produces similar equilibrium branches, except that its equivalent of branch 1 is a flat branch over δr ± 30 deg, changing from S to L as δr becomes positive (Fig. 4). That is, we have not found it possible to effect a jump from branch 1, the region of equilibrium flat spin, to the less stable oscillatory spin branches and ultimately to trim, by using aerodynamic controls. Our experience using BACTM thus corroborates qualitatively actual F-4 flight test experience[19] in which it was found that flat spin recovery could be achieved only by using wing-tip rockets or parachutes. Because BACTM curves are global and inexpensively obtained, our methodology offers potential for reducing costs in preliminary design configuration studies. The global nature of BACTM is demonstrated in Fig. 2, when one realizes that the standard analysis approaches are limited to the (linear) S segment on branch 3 which surrounds point B. Accuracy of predictions is limited by the simulation model of the aircraft and not by the method itself. Developing sufficient confidence in high-α models is, and remains, a difficult goal.

Figure 5 shows yaw rate limit cycle amplitude as a function of rudder for the aircraft F model. Limit cycle amplitude is computed as the difference between maximum and minimum values of a variable, such as yaw rate, in a limit cycle condition. Here, aileron and elevator are fixed at 15 and 0 deg, respectively. Note that there are two branches (limit cycles) for some values of δr, but that one is unstable. It "annihilates" the stable branch at $\delta r = 28$ deg, a global bifurcation. The figure shows that for $\delta r > 28$ deg, there is no limit cycle motion; if fixed-point equilibria exist here, they must be found by the appropriate BACTM algorithms. Stability is determined by the criteria applicable to closed orbits,

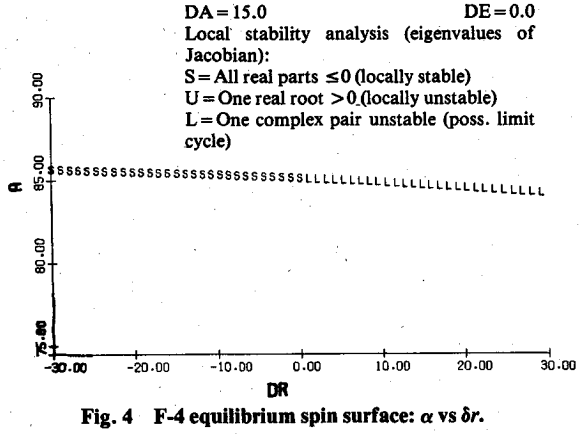

Fig. 4 F-4 equilibrium spin surface: α vs δr.

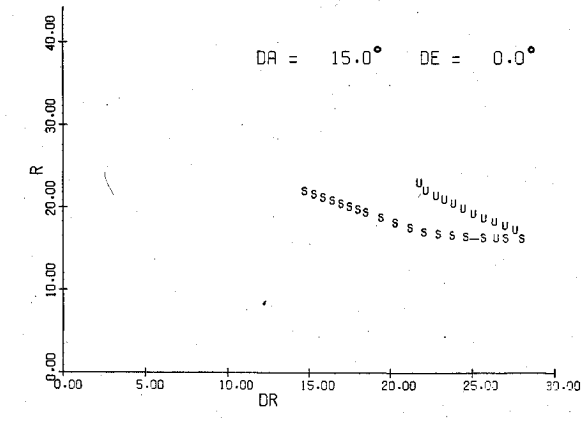

Fig. 5 Aircraft F yaw rate limit cycle amplitude vs δr.

discussed in Sec. III. The limit cycle period T also varies as a function of δr, with values between 2 and 3 seconds for this example. BACTM simultaneously generates solutions like Fig. 5 for all of the state variables, plus T. Means of the state variables, as well as amplitudes, may also be plotted.

Bifurcation surfaces combine with equilibrium surfaces to provide a powerful analysis tool. The number of equilibrium solutions changes as one crosses a bifurcation surface boundary (i.e., jumps occur). In Fig. 6 a part of the F-4 bifurcation surface is shown in the $\delta a - \delta r$ plane, with $\delta e = -3.5$ deg. The numbers in some of the regions indicate the number of equilibria (stable and unstable) for that region. The utility of surfaces such as these lies in the fact that autopilot synthesis can be greatly aided. For example, most aileron-rudder interconnect systems use a simple linear relationship $\delta a = k\delta r$, where k is a constant. A more natural approach, based on such curves as the one shown in Fig. 6, is to construct a more general interconnect relationship, say $\delta r = k_0 + k_1\delta a + k_2\delta a^2$, which would specify allowed deflections. Or, one could mechanize scheduled deflection limits for the controls as a means of preventing control sequences whose loci would traverse a critical boundary in Fig. 6. Such limits would define a stability envelope for the region of interest, and it is conceivable that such an envelope would provide the pilot with more control freedom than a control-interconnect system derived without the insight into the steady-state dynamics provided by BACTM. We emphasize here, however, that BACTM neither quantifies nor predicts transient motion, or motion induced by rapid, large-order control deflections. The curves described above can predict steady-state or equilibrium behavior. Furthermore, this behavior is quantified only for motions attracted to stable equilibria; motion initiating near an unstable equilibrium (fixed point or fixed orbit) "goes elsewhere."

Finally, BACTM analysis has confirmed the presence of Hopf bifurcation phenomena in high-α aircraft dynamics. Essentially, a Hopf bifurcation marks the bifurcation to a limit cycle motion from a stable equilibrium condition, as the parameter λ passes a critical value. The most common example of this in high-α dynamics occurs during a pitch up maneuver, in which equilibrium α increases from trim values (about 3 deg) through its stall value (about 12-14 deg at subsonic speeds for the F-4). As α increases, the motion changes from stable to prestall buffeting to wing rock, completing the Hopf bifurcation. Quite often, the S-to-L transition on an equilibrium surface indicates a Hopf bifurcation; at this time,

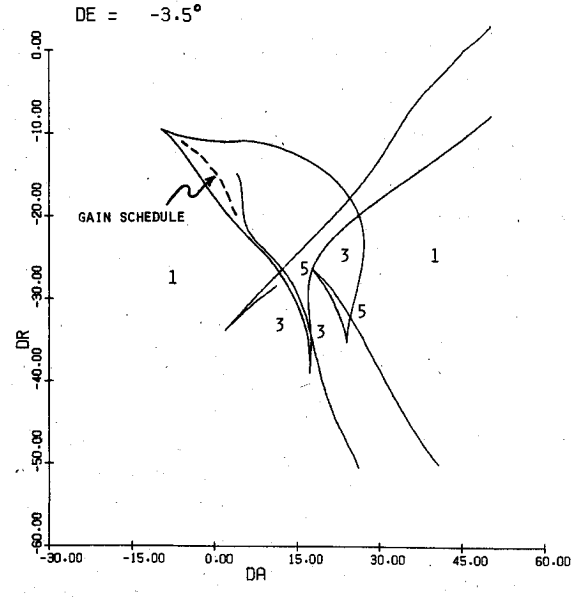

Fig. 6 F-4 bifurcation surface, $\delta e = -3.5$ deg.

we must verify such a conjecture using time history simulations or limit cycle computations of Sec. III. We are, however, incorporating an algorithm developed by Hassard et al.[28] This algorithm finds the critical value of λ and computes limit cycle period and stability at critical λ.

V. Conclusions

Based on analysis of the nonlinear models of the F-4 and aircraft F, we can conclude that:

1) A large number of unstable, jump, and limit cycle phenomena occurring at high angles of attack, can be analyzed in a unified fashion by using the high-α bifurcation analysis and catastrophe theory methodology.

2) The methodology provides a global representation of the equilibrium and bifurcation surfaces for nonlinear dynamic systems. The qualitative dynamics of the system for different initial conditions, controls, and system parameters can be obtained easily from the equilibrium and bifurcation surfaces. In particular, the control and parameter values for which jumps and limit cycles appear are obtained directly from the equilibrium and bifurcation surfaces. The method also provides insights into the control and identification problems for nonlinear dynamic systems.

3) Our method can generate equilibrium surfaces for aircraft models whose aerodynamic data are available in three main classes over wide ranges of angle of attack and sideslip angle. Based on these surfaces, elementary control strategies for spin recovery have been developed, and these agree well with more optimum flight recovery procedures. In addition, the equilibrium surfaces have provided a basis for study of other high-α phenomena such as stall, wing rock, and poststall oscillatory motions.

4) We have indicated how the methodology may be used to synthesize a command augmentation system for the F-4, using its bifurcation surfaces along with the criterion of maximizing the range of control values which avoid jump or limit cycle behavior.

5) The bifurcation analysis methodology has been expanded to include quantitative detection and analysis of limit cycle motions, and the generation of limit cycle solution points by means of continuation methods. Limit cycle stability information is also obtained.

6) F-4 analysis has provided qualitative confirmation of behavior which has been determined beforehand using more exhaustive approaches. When correlation between aircraft models based on wind-tunnel data and flight test results is improved, the methodology will provide useful quantative results on actual performance, as well as represent a basis for analyzing the effect of configuration or parameter changes made to the aircraft.

The methodology presented here, and the manner in which it has been extended to complicated, nonlinear, high-order systems through the use of numerical techniques based on parametric continuation, adds to the flight dynamics analyst's repertoire a significant new tool. This methodology provides not only quantitative global stability information, but also the capability to predict and explain such nonintuitive phenomena as jumps, limit cycles, and hysteresis, and to develop guidelines for stabilizing an unstable nonlinear system. In particular, for aircraft, the location and characteristics of the dynamic stability envelope can be determined more effectively, thereby reducing artificial constraints on the aircraft's control effectiveness.

The advances in providing quantitative information on limit cycles—their location, stability, and parametric dependence—are potentially of great value to aircraft designers. This is not only because so much of the critical aircraft nonlinear phenomena is oscillatory, but also because currently available techniques are incapable of providing adequate information globally. Frequency domain, eigenvector, and describing function techniques provide in the high-α domain only limited localized information, and they usually require very restricted, quasilinear models which can obscure important phenomena. The new approach makes no such a priori demands on the model, only that it be sufficiently continuous in the state variables.

Acknowledgment

This research was supported by the Office of Naval Research under Contracts N00014-76-C-0780 and N00014-79-C-0705.

References

[1] Chambers, J.R., "Status of Model Testing Techniques," Paper presented at the AFFDL Stall/Post-Stall/Spin Symposium, Dec. 1971.

[2] Campbell, J., "A Technique Utilizing Free Flying Radio-Controlled Models to Study Incipient- and Developed-Spin Characteristics of Airplanes," AGARD Rept. 76, 1959.

[3] Takens, F., "Introduction to Global Analysis," and "Notes on Forced Oscillations," *Communications 2 and 3, Mathematical Institute Rijksuniversiteit,* Utrecht, The Netherlands, 1973.

[4] Thom, R., *Structural Stability and Morphogenesis,* Addison-Wesley, Reading, Mass., 1974, pp. 47, 48, 55-92.

[5] Stengel, R.F., Taylor, J.H., Broussard, J.R., and Berry, P.W., "High Angle-of-Attack Stability and Control," Office of Naval Research, Rept. ONR-CR-215-237-1, 1976.

[6] Hall, W.E., Gupta, N.K., and Tyler, J.S., "Model Structure Determination and Parameter Identification for Nonlinear Aerodynamic Flight Regimes," *Methods for Aircraft State and Parameter Identification,* AGARD-CP-712, 1974.

[7] Keller, H.B., "Numerical Solution of Bifurcation and Nonlinear Eigenvalue Problems," *Applications of Bifurcation Theory,* edited by P.H. Rabinowitz, Academic Press, New York, 1977, pp. 359-384.

[8] Rheinboldt, W.C., "An Adaptive Continuation Process for Solving Systems of Nonlinear Equations," University of Maryland, Computer Sciences Tech. Rept. TR-393, 1975.

[9] Kubicek, M., "Algorithm 502, Dependence of Solution of Nonlinear Systems on a Parameter," *ACM-TOMS,* Vol. 2, pp. 98-107, 1976.

[10] Chua, L.O. and Lin, P.M., *Computer-Aided Analysis of Electronic Circuits,* Prentice-Hall, Englewood Cliffs, N.J., 1975, pp. 697-702.

[11] Mehra, R.K., "Catastrophe Theory, Nonlinear System Identification and Bifurcation Control," *Proceedings of Joint Automatic Control Conference,* 1976, pp. 823-831.

[12] Schy, A.A. and Hannah, M.E., "Prediction of Jump Phenomena in Rolling Coupled Maneuvers of Airplanes," *Journal of Aircraft,* Vol. 14, April 1977, pp. 375-382.

[13] Young, J.W., Schy, A.A., and Johnson, K.G., "Pseudosteady-State Analysis of Nonlinear Aircraft Maneuvers," NASA TP-1758, Dec. 1980.

[14] Davidenko, D., "On a New Method of Numerically Integrating a System of Nonlinear Equation," *Doklady Akademii Nauk, SSSR,* Vol. 88, 1953, pp. 601-604 (in Russian).

[15] Lahaye, E., "Une Methode de Resolution d'une Categorie d'Equations Transcendates," *Comptes Rendus de 'Academie de Sciences,* Paris, Vol. 198, 1934, pp. 1840-1842.

[16] Klopfenstein, R.W., "Zeroes of Nonlinear Functions," *Journal of ACM,* Vol. 8, 1961, pp. 366-373.

[17] Adams, W.M., "Analytic Prediction of Airplane Equilibrium Spin Characteristics," NASA TN D-6926, 1972.

[18] Moore, F.L., Anglin, E.L., Adams, M.S., Deal, P.L., and Person, L.H., "Utilization of a Fixed-Base Simulation to Study the Stall and Spin of Fighter Airplanes," NASA TN D-6117, 1971.

[19] Rutan, E.L., McElroy, E.C., and Gentry, J.R., "Stall/Near Stall Investigation of the F-4 Aircraft," U.S. Air Force Flight Test Center, Tech. Rept. 70-20, 1970.

[20] Mehra, R.K., Kessel, W.C., and Carroll, J.V., "Global Stability and Control Analysis of Aircraft at High Angles-of-Attack," Rept. ONR-CR-215-248-1, 1977.

[21] Mehra, R.K., Washburn, R.B., Sajan, S., and Carroll, J.V., "A Study of the Application of Singular Perturbation Theory," NASA CR-3167, 1979.

[22] Holmes, P.J. and Marsden J., "Bifurcation to Divergence and Flutter in Flow-Induced Oscillations: An Infinite-Dimensional Analysis," *Automatica,* Vol. 14, 1978, pp. 367-384.

[23] Howard, L.N., "Bifurcations in Reaction-Diffusion Problems," *Advances in Mathematics,* Vol. 16, No. 2, May 1975, pp. 246-258.

[24] Abraham, R. and Marsden, J.E., *Foundations of Mechanics,* Benjamin/Cummings, Reading, Mass., 1978, pp. 489-571.

[25] Casti, J.L., *Connectivity, Complexity and Catastrophe in Large-Scale Systems,* John Wiley & Sons, New York, 1979, pp. 126-200.

[26] Hirsch, M. and Smale, S., *Differential Equations, Dynamical Systems and Linear Algebra,* Academic Press, New York, 1974, pp. 276-286.

[27] Rinzel, J. and Miller, R.N., "Numerical Calculation of Stable and Unstable Periodic Solutions to the Hodgkin-Huxley Equations," *Mathematical Biosciences,* Vol. 49, 1980, pp. 27-59.

[28] Hassard, B.D., "Theory and Applications of Hopf Bifurcation," *London Mathematical Society, Lecture Note Series No. 41,* Cambridge University Press, Cambridge, England, 1981, pp. 1-85, 129-180.